

Mineralization of the antibiotic chloramphenicol by solar photoelectro-Fenton.

From stirred tank reactor to solar pre-pilot plant



Sergi Garcia-Segura^a, Eliane Bezerra Cavalcanti^b, Enric Brillas^{a,*}

^a Laboratori d'Electroquímica dels Materials i del Medi Ambient, Departament de Química Física, Facultat de Química, Universitat de Barcelona, Martí i Franquès 1–11, 08028 Barcelona, Spain

^b Instituto de Tecnología e Pesquisa/ITP, Universidade Tiradentes/UNIT, Av. Murilo Dantas 300, CEP 49032-490 Aracaju, SE, Brazil

ARTICLE INFO

Article history:

Received 2 July 2013

Received in revised form 27 July 2013

Accepted 30 July 2013

Available online 9 August 2013

Keywords:

Antibiotics

Oxidation products

Solar photoelectro-Fenton

Solar photolysis

Water treatment

ABSTRACT

Chloramphenicol is a widely used broad-spectrum antibiotic, which has been detected as emerging pollutant in natural waters. The mineralization of this drug in a synthetic sulfate solution of pH 3.0 has been studied by anodic oxidation with electrogenerated H₂O₂ (AO-H₂O₂), electro-Fenton (EF), UVA photoelectro-Fenton (PEF) and solar photoelectro-Fenton (SPEF). Comparative electrolyses carried out with 100 mL stirred tank reactors equipped with a boron-doped diamond (BDD) or Pt anode and an air-diffusion cathode at constant current density showed the superiority of the processes with BDD because of the higher oxidation ability of •OH formed from water oxidation at the BDD surface. Total mineralization was rapidly reached for the most potent treatment of SPEF with BDD due to the additional oxidation by •OH produced from Fenton's reaction between added Fe²⁺ (0.5 mM) and H₂O₂ generated at the cathode, together the synergistic photolytic action of sunlight, much more intense than the 6 W UVA lamp used in PEF. Chloramphenicol decay always followed a pseudo-first-order kinetics. The influence of current density and substrate concentration on SPEF with BDD was examined. Nine aromatic products, thirteen hydroxylated derivatives and seven carboxylic acids were identified by different chromatographic techniques. While the initial Cl of the drug was released as chloride ion, its initial N was lost as nitrate ion and, in smaller proportion, as ammonium ion. From the detected products, a general reaction pathway for chloramphenicol mineralization is proposed. The viability of SPEF was confirmed in a 10 L pre-pilot plant with a Pt/air-diffusion filter-press reactor coupled to a solar CPCs photoreactor. After 180 min of electrolysis at 100 mA cm⁻², a 245 mg L⁻¹ chloramphenicol solution in 0.05 M Na₂SO₄ with 0.5 mM Fe²⁺ at pH 3.0 underwent 89% mineralization with 36% current efficiency and 30.8 kWh m⁻³ energy cost.

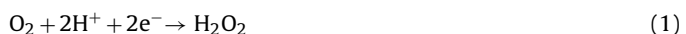
© 2013 Elsevier B.V. All rights reserved.

1. Introduction

Recently, there exists an increasing attention on pharmaceuticals as potential bioactive chemicals in the aquatic environment. Many pharmaceutical drugs have been detected at relatively low contents up to $\mu\text{g L}^{-1}$ level in soils, surface waters, ground waters and even drinking waters [1–3]. Antibiotics are the most commonly drugs found in the aquatic environment because their antimicrobial nature prevents effective removal in sewage treatment plants [4–6]. The occurrence and fate of antibiotics as well as their metabolites in water streams is recognized as one of the emerging issues in environmental chemistry [1,3,7,8]. Several authors reported that these pollutants can produce multi-resistant strains of microorganisms, can affect the endocrine systems of fishes

and invertebrates, and are toxic on small invertebrates and algae [9–12]. Powerful oxidation treatments then need to be developed for the removal of antibiotics from waters and wastewaters to avoid their potential adverse health effects on humans and animals.

Several electrochemical advanced oxidation processes (EAOPs) are being currently developed for water prevention [12–17]. EAOPs are based on the *in situ* generation of hydroxyl radical (•OH), which is the second strongest oxidant known after fluorine since it has so high standard reduction potential ($E^\circ(\bullet\text{OH}/\text{H}_2\text{O}) = 2.80 \text{ V/SHE}$) that can non-selectively react with organic pollutants up to their mineralization to CO₂, water and inorganic ions. The most potent EAOPs use both, heterogeneous and homogeneous •OH formed at the anode and in the solution bulk, respectively, as oxidizing agents. Mediated electro-oxidation with homogeneous •OH is usually achieved by decomposition of H₂O₂ generated from the two-electron cathodic reduction of injected O₂ [12,16]:



* Corresponding author. Tel.: +34 93 4021223; fax: +34 93 4021231.

E-mail address: brillas@ub.edu (E. Brillas).

Good efficiencies for H₂O₂ generation from reaction (1) have been reported for carbonaceous cathodes such as carbon sponge [18], carbon nanotubes-polytetrafluoroethylene (PTFE) [19,20], carbon-felt [18,21–25], graphite-felt [26], boron-doped diamond (BDD) [27] and carbon-PTFE gas (O₂ or air) diffusion electrodes [21,22,28–32].

In our laboratory, we have checked the good oxidation ability of EAOPs like anodic oxidation with electrogenerated H₂O₂ (AO-H₂O₂) [28,32], electro-Fenton (EF) [21,22,28–31], UVA photoelectro-Fenton (PEF) [28–30] and solar photoelectro-Fenton (SPEF) [29,31] to destroy several antibiotics and other drugs in acidic solutions using small stirred tank reactors equipped with either a BDD or Pt anode and a gas-diffusion cathode. Our interest is to show that these EAOPs can be useful for the treatment of wastewaters contaminated with antibiotics. To do this and in view of the large variety of these drugs, it is necessary to know the degradative characteristics of more compounds. In this way, the scaling-up of EAOPs to a pre-pilot plant also needs to be assessed in order to demonstrate their possible viability at industrial level.

This paper aims to investigate the mineralization of the antibiotic chloramphenicol (2,2-dichloro-N-[1,3-dihydroxy-1-(4-nitrophenyl)propan-2-yl] acetamide) in acidic medium by AO-H₂O₂, EF, PEF and SPEF in order to clarify: (i) the role of generated •OH in the degradative processes using stirred Pt/air-diffusion and BDD/air-diffusion tank reactors of 100 mL under comparable conditions, (ii) the photolytic action of UVA and solar radiation in these systems, (iii) the effect of experimental parameters on substrate decay and mineralization rate, (iv) the products formed and their evolution to propose a general reaction pathway for chloramphenicol mineralization and (v) the viability of SPEF in a 10 L pre-pilot plant with a Pt/air-diffusion filter-press reactor coupled to a solar compound parabolic collectors (CPCs) photoreactor. Note that chloramphenicol is a broad-spectrum antibiotic, which is effective against a wide variety of Gram-positive and Gram-negative bacteria, including most anaerobic organisms. While in the developed countries it is currently prescribed only to treat bacterial conjunctivitis, chloramphenicol is widely used in developing countries. For this reason, it has been detected worldwide in ground waters, lakes, rivers and influents and effluents of sewage treatment plants [3,6–8,33–36]. However, less is known about the degradation of chloramphenicol from waters and its oxidation products formed from •OH attack have not been identified yet. It has been reported that it can be removed by UVC radiation [37], TiO₂/UV photocatalysis [38] and ozonation [39]. The electrochemical reduction of its nitro group to hydroxylamine or amine at a graphite cathode has also been described by means of cyclic voltammetry [40].

2. Experimental

2.1. Chemicals

Chloramphenicol (98% purity) was of reagent grade from Sigma-Aldrich. Carboxylic acids were of reagent grade from Panreac and Avocado. Anhydrous sodium sulfate and heptahydrated ferrous sulfate were of analytical grade from Fluka. Solutions treated in the stirred tank reactor were prepared with ultrapure water obtained from a Millipore Milli-Q system (resistivity > 18 MΩ cm at 25 °C). Solutions of 10 L to be degraded in the solar pre-pilot plant were prepared with deionized water. All solutions were adjusted to pH 3.0 with analytical grade sulfuric acid purchased from Merck. Other chemicals employed were of LC-MS, HPLC or analytical grade from Merck, Panreac and Sigma-Aldrich.

2.2. Electrochemical and photoelectrochemical systems

Experiments with 100 mL solutions were conducted in an undivided and cylindrical stirred tank reactor, with a double jacket in which external water circulated to maintain the solution temperature at 35 °C. The anode was either a BDD thin film electrode provided by Adamant Technologies or a Pt sheet of 99.99% purity supplied by SEMPSA. The cathode was a carbon-PTFE air-diffusion electrode purchased from E-TEK. The preparation of this cathode was described elsewhere [41] and was fed with air pumped at 300 mL min⁻¹ for H₂O₂ generation from reaction (1). The area of both electrodes was 3 cm² and the interelectrode gap was ca. 1 cm. To remove the impurities of the BDD surface and activate the air-diffusion cathode prior use, they were polarized in 0.05 M Na₂SO₄ at 100 mA cm⁻² for 60 min. All trials were carried out under vigorous stirring with a magnetic bar at 800 rpm to ensure homogenization and the transport of reactants toward/from the electrodes. For the PEF assays, a Philips 6-W black light blue tube was placed at 7 cm above the solution. This lamp emitted UVA light between 320 and 400 nm with $\lambda_{\text{max}} = 360$ nm, yielding a photoionization energy of 5 W m⁻² as detected with a Kipp & Zonen CUV 5 global UV radiometer. In the SPEF assays, the tank reactor was directly exposed to solar radiation with a mirror placed at its bottom to better collect the sun rays.

A scheme of the solar pre-pilot plant operating in batch circulation mode was presented elsewhere [42]. For each EF or SPEF trial, the solution was introduced in the reservoir and continuously recirculated by a peristaltic pump at a flow rate of 200 L h⁻¹ adjusted by a rotameter. The temperature was maintained at 35 °C by two heat exchangers. The electrolytic cell was an undivided filter-press reactor equipped with a Pt sheet anode from SEMPSA and a carbon-PTFE air-diffusion cathode from E-TEK. A PVC liquid compartment with a central window of 9.5 cm × 9.5 cm (90.2 cm²) was used to contact the effluent with the outer faces of both electrodes, separated 1.2 cm. The inner face of the cathode was pressed to a Ni mesh as electrical connector in contact with a PVC gas chamber where circulated compressed air at a flow rate of 4.5 L min⁻¹ regulated with a back-pressure gauge. The solar CPCs photoreactor with an area of 0.4 m² and concentration factor of 1 was composed of twelve borosilicate-glass tubes of 50.5 cm length × 1.82 cm inner diameter (irradiated volume 1.57 L), with connecting tubing and valves mounted in an aluminum frame on a platform tilted 41° to better collect the direct sun rays in our laboratory of Barcelona (latitude: 41°21'N, longitude: 2°10'E). In EF, the solar CPCs photoreactor was coated with a black plastic.

All solar trials were made for 240 min as maximal in sunny and clear days during summer 2012. The average solar UV radiation intensity (between 300 and 400 nm) was 30–32 W m⁻², as measured with a Kipp & Zonen CUV 5 global UV radiometer.

2.3. Apparatus and analytical procedures

The solution pH was measured with a Crison GLP 22 pH-meter. Galvanostatic electrolyses were performed with an Amel 2051 potentiostat-galvanostat for the tank reactor experiences and a Grelco GDL3020 power supply for the assays with the solar pre-pilot plant. Aliquots of 1 mL were withdrawn from electrolyzed solutions and filtered with 0.45 µm PTFE filters from Whatman before analysis. The mineralization of chloramphenicol solutions was monitored from their dissolved organic carbon (DOC) abatement, determined on a Shimadzu TOC-VCSN analyzer. Reproducible DOC values with an accuracy of ±1% were obtained by injecting 50 µL aliquots to the analyzer. Total nitrogen (TN) was determined with a Shimadzu TNM-1 unit coupled with the TOC analyzer.

The chloramphenicol decay was followed by reversed-phase HPLC using a Waters 600 LC fitted with a Spherisorb ODS2 5 µm (150 mm × 4.6 mm) column at 35 °C and coupled with a Waters 996 photodiode array detector selected at $\lambda = 278.2$ nm. Carboxylic acids were detected by ion-exclusion HPLC using the above LC fitted with a Bio-Rad Aminex HPX 87H (300 mm × 7.8 mm) column at 35 °C and the photodiode array detector set at $\lambda = 210$ nm. In the HPLC measurements, 20 µL aliquots were injected into the chromatograph and the mobile phase was either a 20:80 (v/v) acetonitrile/phosphate buffer (pH=3.5) mixture at 0.4 mL min⁻¹ for reversed-phase HPLC or 4 mM H₂SO₄ at 0.6 mL min⁻¹ for ion-exclusion HPLC. The inorganic ions were quantified by ion chromatography using a Shimadzu 10 Avp HPLC coupled with a Shimadzu CDD 10 Avp conductivity detector. The NH₄⁺ content was obtained with a Shodex IC YK-421 (125 mm × 4.6 mm) cation column at 40 °C, whereas the NO₃⁻ and Cl⁻ contents were determined with a Shim-Pack IC-A1S (100 mm × 4.6 mm) anion column at 40 °C. These analyses were made by injecting 25 µL aliquots and using mobile phases composed of a 5.0 mM tartaric acid, 1.0 mM dipicolinic acid, 24.2 mM boric acid and 1.5 mM crown ether solution at 0.8 mL min⁻¹ for NH₄⁺ and a 2.4 mM tris(hydroxymethyl)aminomethane and 2.5 mM phthalic acid solution of pH 4.0 at 1.5 mL min⁻¹ for NO₃⁻ and Cl⁻.

Products formed after 5–20 min of EF treatment of a 245 mg L⁻¹ chloramphenicol solution in a BDD/air-diffusion tank reactor at 33.3 mA cm⁻² were identified by LC-MS using a Shimadzu SIL-20AC LC coupled to a Shimadzu LCMS-2020 MS. The LC was fitted with a Teknokroma Mediterranean Sea C-18 3 µm (15 mm × 0.46 mm) column at 30 °C. The MS operated in the negative and positive modes with electrospray source ionization (ESI), by applying an interface voltage of -4.5 and 4.5 kV, respectively, and 60 V Q-array RF voltage. The DL temperature was 250 °C and pure N₂ was used as nebulising and dryer gas. Mass spectra were collected in the *m/z* range 50–420 using total ion current (TIC) acquisition. For these analyses, 15 µL aliquots were introduced into the LC, previously filtered with a Millipore filter of 0.22 µm, and the mobile phase was a 75:25 (v/v) acetonitrile/water (5.0 mM ammonium acetate) mixture at 0.2 mL min⁻¹.

3. Results and discussion

3.1. Comparative mineralization of chloramphenicol by EAOPs in a stirred tank reactor

The relative oxidation ability of AO-H₂O₂, EF, PEF and SPEF to destroy chloramphenicol was assessed by electrolyzing 100 mL of a synthetic solution with 245 mg L⁻¹ drug (100 mg L⁻¹ of DOC) and 0.05 M Na₂SO₄ at pH 3.0 using stirred Pt/air-diffusion and BDD/air-diffusion tank reactors at 33.3 mA cm⁻² and 35 °C. The pH of 3.0 was chosen because it was found optimal for the treatment of other aromatics by these EAOPs [12,28–31] and treatments were made at 35 °C since this is the maximum temperature allowed in the open tank reactor without significant water evaporation from the solution during prolonged electrolysis [41]. For EF, PEF and SPEF, 0.5 mM Fe²⁺ was also added to the solution, which is the best catalyst concentration found for these processes under the conditions tested [28–31]. The chloramphenicol concentration checked was much higher than the usually detected in wastewaters, simply to better evaluate its mineralization behavior and identify its degradation products, as will be discussed below. In all these trials, the solution pH remained practically unchanged and decayed to values 2.7–2.8 after 360 min of the longer treatments, probably due to the formation of acidic products like short-chain carboxylic acids [12,16]. The cell voltage for BDD (17.0 V) was much higher than for Pt (8.3 V).

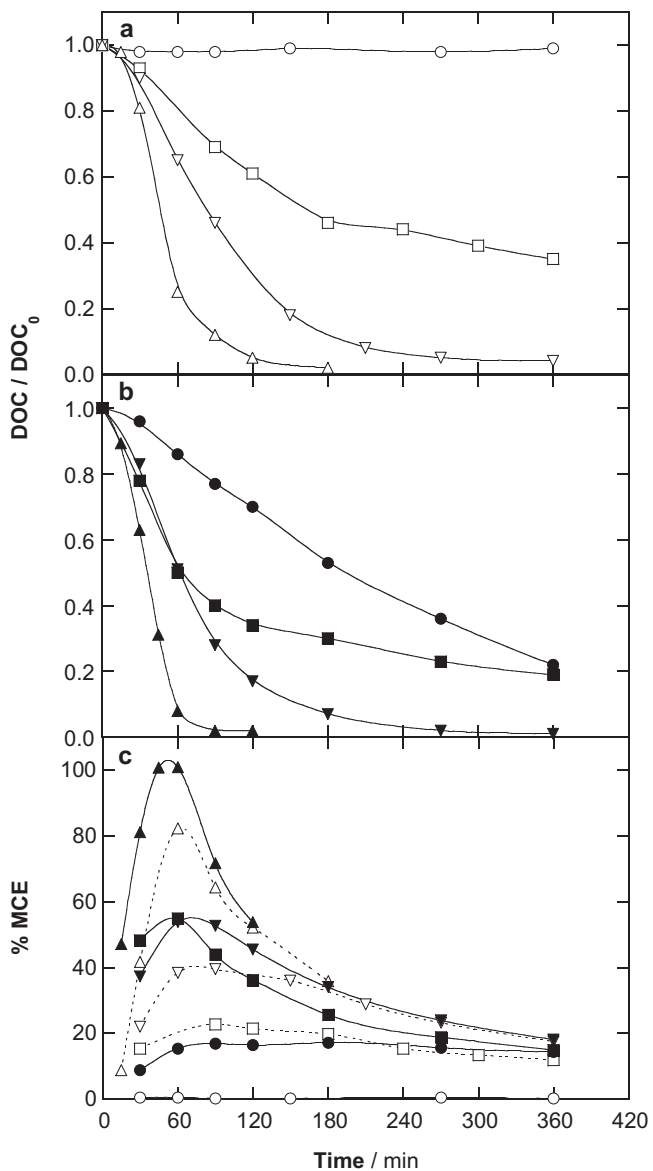
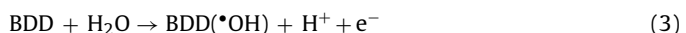


Fig. 1. Normalized DOC abatement with electrolysis time for the (○, ●) AO-H₂O₂, (□, ■) EF, (▽, ▼) PEF with a 6 W UVA light and (△, ▲) SPEF treatment of 100 mL of 245 mg L⁻¹ chloramphenicol in 0.05 M Na₂SO₄ at pH 3.0, 33.3 mA cm⁻² and 35 °C. In the three latter methods, the solution also contained 0.5 mM Fe²⁺. (a) Pt/air-diffusion and (b) BDD/air-diffusion tank reactor. Plot (c) presents the mineralization current efficiency for the trials.

Fig. 1a and **b** depicts the change of normalized DOC for the above trials. For each EAOP, the chloramphenicol solution was more rapidly mineralized using a BDD than a Pt anode. In both systems, the relative oxidation ability of processes rose following the sequence AO-H₂O₂ < EF < PEF < SPEF. The lowest mineralization was achieved for AO-H₂O₂ because organics can only be slowly degraded by physisorbed Pt([•]OH) or BDD([•]OH) radicals formed from water oxidation at the Pt or BDD anode surface by reactions (2) and (3), respectively [15,28]:



The expected higher oxidation ability of BDD([•]OH) than Pt([•]OH) [15] then explains that the solution became more largely mineralized with a BDD anode. In fact, DOC was not practically removed

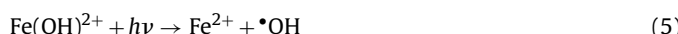
in the Pt/air-diffusion tank reactor (see Fig. 1a), whereas it was reduced by 78% at 360 min in the BDD/air-diffusion one (see Fig. 1b).

The mineralization rate of chloramphenicol increased in EF owe to the additional oxidative action of large amounts of •OH produced in the bulk from Fenton's reaction (4) between added Fe²⁺ and electrogenerated H₂O₂ [12,16,23,29]:



This reaction is catalytic and can be continuously propagated mainly from Fe³⁺ reduction to Fe²⁺ at the cathode. The fast reaction of organics with •OH can be confirmed in Fig. 1a, showing that DOC decayed up to 65% at the end of EF with Pt. The same behavior can be seen in Fig. 1b for EF with BDD, although in this case 81% of DOC was finally removed, a value very close to that of AO-H₂O₂ treatment. This can be related to the formation of Fe(III)-carboxylate complexes that are hardly destroyed by BDD(•OH) and •OH [21,28–31].

The chloramphenicol mineralization was more largely accelerated under UVA radiation with a 6-W light in PEF. This synergistic action can be related to two phenomena: (i) the photolysis of Fe(OH)²⁺, the pre-eminent Fe³⁺ species near pH 3, regenerating Fe²⁺ and producing more •OH from reaction (5) and (ii) the photodecarboxylation of some generated Fe(III)-carboxylate species according to the general reaction (6) [12,16].



The quick photolysis of Fe(III)-carboxylate species can then justify the almost total mineralization (96% DOC decay) and total mineralization (99% DOC decay) found for PEF with Pt and BDD, respectively. Fig. 1a and b also shows that the use of SPEF is much more effective, attaining total mineralization (98% DOC abatement) at 180 and 120 min of electrolysis using the Pt/air-diffusion and BDD/air-diffusion tank reactors, respectively. The greater UVA intensity of sunlight (about 30 W m⁻²) in PEF than of the 6-W lamp (5 W m⁻²) in SPEF can justify the superiority of the former process. The highest oxidation ability of SPEF with BDD is then due to the quickest destruction of organics under the synergistic action of BDD(•OH), •OH and sunlight.

For the above trials, the corresponding mineralization current efficiency (MCE) at given electrolysis time (*t*, in h) was estimated by the following equation [29]:

$$\text{MCE}(\%) = \frac{nFV_s \Delta(\text{DOC})_{\text{exp}}}{4.32 \times 10^7 mIt} 100 \quad (7)$$

where *F* is the Faraday constant (96487 C mol⁻¹), *V_s* is the solution volume (L), $\Delta(\text{DOC})_{\text{exp}}$ is the experimental DOC decay (mg L⁻¹), 4.32×10^7 is a conversion factor to homogenize units (3600 s h⁻¹ × 12,000 mg mol⁻¹), *m* is the number of carbon atoms of chloramphenicol (11 carbon atoms) and *I* is the applied current (A). The number *n* of electrons consumed per chloramphenicol molecule was taken as 54 from reaction (8) considering its mineralization to CO₂ with loss of NO₃⁻ and Cl⁻ as main primary inorganic ions, as discussed below.

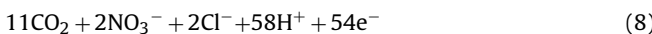


Fig. 1c highlights the rise in MCE of the EAOPs tested in each system according to their relative oxidation ability, as well as the greater efficiency for all processes with BDD compared with the corresponding treatments with Pt. As expected, SPEF with BDD led to the highest MCE, with a maximum value near 100% between 45 and 60 min of electrolysis, further diminishing to 53% at 120 min.

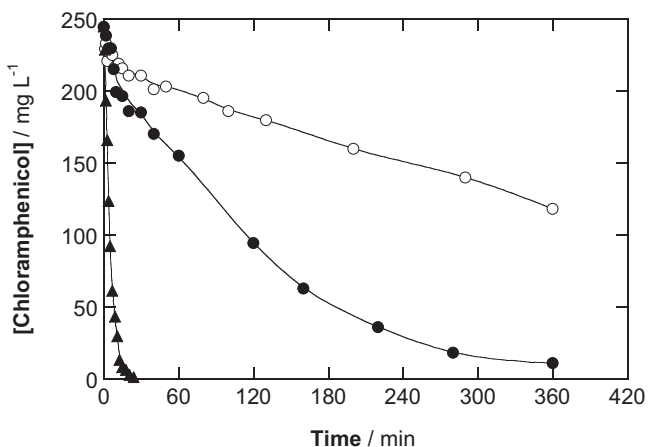


Fig. 2. Chloramphenicol concentration decay vs electrolysis time for the (○, ●) AO-H₂O₂ and (▲, ■) SPEF degradations under the conditions of Fig. 1 using a (○) Pt/air-diffusion or (●, ■) BDD/air-diffusion tank reactor.

For most processes, maximum efficiency at short time, followed by its progressive loss with prolonging electrolysis, was also found. This decay in MCE can be accounted for by the presence of less organic matter as well as the gradual formation of more difficultly oxidizable products like short-chain carboxylic acids [12,15,16].

The role of Pt(•OH), BDD(•OH) and •OH was clarified by determining the kinetics of chloramphenicol decay in the above treatments by reversed-phase HPLC, where it displayed a well-defined peak with retention time (*t_r*) of 8.05 min. Blank experiments under direct UVA radiation without electrolysis corroborated that the drug was not directly photolyzed. Fig. 2 evidences a very slow removal of chloramphenicol concentration under the action of Pt(•OH), only passing from 245 to 118 mg L⁻¹ in 360 min, whereas at the same time it was practically completely removed by BDD(•OH). This behavior confirms the much higher oxidation ability of BDD(•OH) in front of Pt(•OH) to destroy chloramphenicol and its oxidation products. Kinetic analysis of these concentration decays showed that they fit well with a pseudo-first-order reaction (data not shown), yielding an apparent rate constant (*k₁*) of $3.0 \times 10^{-5} \text{ s}^{-1}$ (*R*² = 0.981) for AO-H₂O₂ with Pt, which rose to $1.4 \times 10^{-4} \text{ s}^{-1}$ (*R*² = 0.995) for AO-H₂O₂ with BDD. In contrast, chloramphenicol was much more rapidly removed and with a quite similar rate operating with EF, PEF and SPEF, regardless of the anode used. In all these treatments, the drug disappeared in about 27 min, as exemplified in Fig. 2 for SPEF with BDD. The *k₁* value obtained for the pseudo-first-order kinetics followed by this trial was $2.9 \times 10^{-3} \text{ s}^{-1}$ (*R*² = 0.998). All these findings demonstrate the preponderant action of •OH formed from Fenton's reaction (4) to oxidize not only the substrate, but also the aromatic species that are expected to be generated as its primary products. Besides, the similar decay kinetics determined for EF, PEF and SPEF indicates a low participation of photolytic reaction (5) to produce •OH in the two latter EAOPs. The fact that chloramphenicol is always removed following a pseudo-first-order kinetics suggests its reaction with a constant concentration of generated hydroxyl radicals in each treatment.

3.2. Effect of current density and chloramphenicol content on SPEF with BDD in a stirred tank reactor

The influence of key variable parameters such as current density (*j*) and substrate concentration on the SPEF process using a stirred BDD/air-diffusion tank reactor was examined from the DOC abatement of synthetic antibiotic solutions with 0.05 M Na₂SO₄ and 0.5 mM Fe²⁺ of pH 3.0. Fig. 3a shows the gradual quicker

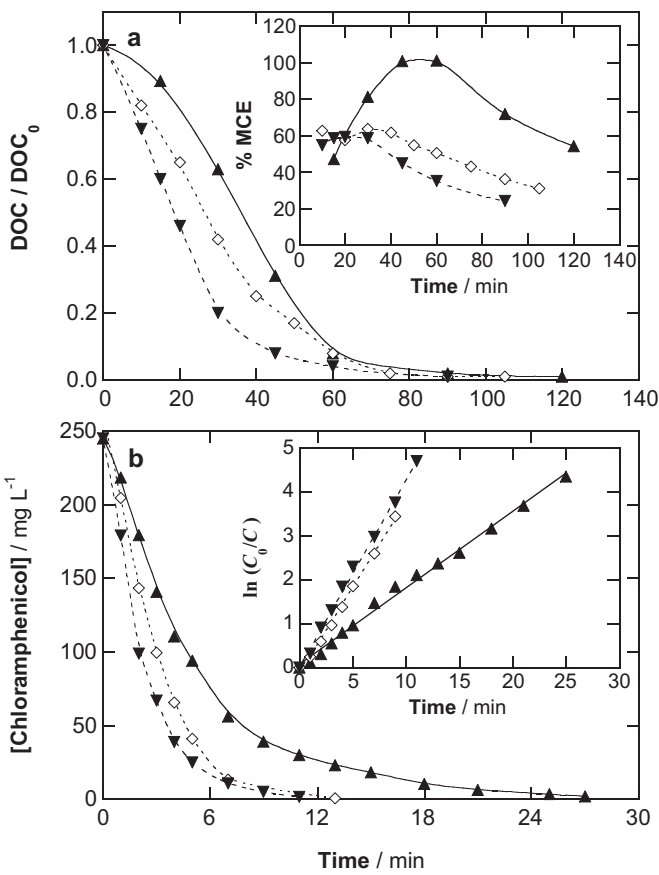


Fig. 3. Effect of current density on (a) normalized DOC removal and (b) substrate concentration abatement with electrolysis time for the degradation of 100 mL of 245 mg L⁻¹ chloramphenicol with 0.05 M Na₂SO₄ and 0.5 mM Fe²⁺ at pH 3.0 and 35 °C by SPEF using a BDD/air-diffusion tank reactor. Applied current density: (▲) 33.3 mA cm⁻², (◇) 66.6 mA cm⁻² and (▼) 100 mA cm⁻². Inset panel: (a) mineralization current efficiency vs electrolysis time and (b) kinetic analysis assuming a pseudo-first-order reaction.

mineralization obtained for 245 mg L⁻¹ chloramphenicol with rising j , attaining total mineralization in 120, 105 and 90 min for 33.3, 66.6 and 100 mA cm⁻², respectively. This trend can be associated with the concomitant increase in rate of all electrode reactions leading to the production of higher amounts of BDD(\bullet OH) from reaction (3) and \bullet OH in the bulk from reaction (4) due to the enhancement of H₂O₂ generation from reaction (1) [43]. The faster destruction of organics with greater quantities of these radicals favors the formation of intermediates that are more rapidly photolyzed by solar radiation, thereby enhancing chloramphenicol mineralization. However, the opposite tendency can be observed in the inset panel of Fig. 3a for the calculated MCE from Eq. (7). Thus, the efficiency dropped as j increased and reached maximum values of 100%, 64% and 59% at 33.3, 66.6 and 100 mA cm⁻², respectively. This loss in efficiency can be related to a gradual loss in the relative quantity of generated BDD(\bullet OH) and \bullet OH due to the higher increase in rate of their non-oxidizing reactions, with the consequent fall in organic events making the mineralization more inefficient. These waste reactions involve primordially the oxidation of BDD(\bullet OH) to O₂ via reaction (9), as well as the dimerization of \bullet OH to H₂O₂ from reaction (10) and its reaction either with Fe²⁺ from reaction (11) or with H₂O₂ generating the weaker oxidant hydroperoxyl radical (HO₂ \bullet) from reaction (12) [15,16,23,30]. The relative amount of generated BDD(\bullet OH) could also fall by the quicker formation of other weaker oxidants at the BDD anode such

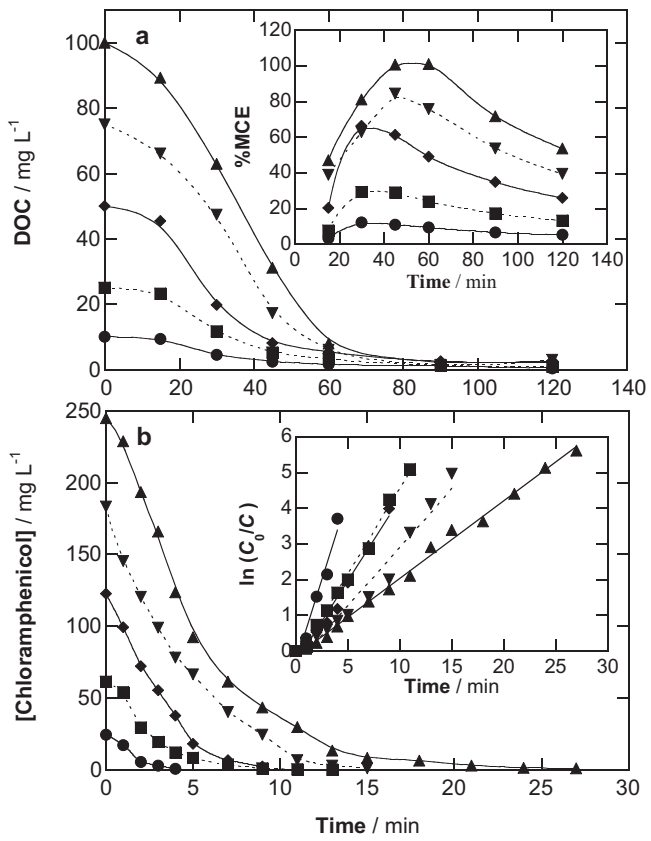
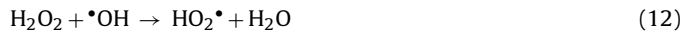
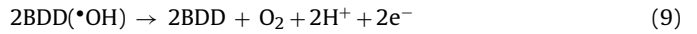


Fig. 4. Influence of initial chloramphenicol concentration on (a) DOC abatement and (b) substrate concentration abatement vs electrolysis time for the SPEF degradation of 100 mL of drug solutions in 0.05 M Na₂SO₄ with 0.5 mM Fe²⁺ at pH 3.0, 33.3 mA cm⁻² and 35 °C using a BDD/air-diffusion tank reactor. Initial DOC content: (●) 24.5 mg L⁻¹, (■) 61.2 mg L⁻¹, (◇) 122.5 mg L⁻¹, (▼) 183.7 mg L⁻¹ and (▲) 245 mg L⁻¹. Inset panel: (a) mineralization current efficiency vs electrolysis time and (b) analysis considering a pseudo-first-order kinetics.

peroxodisulfate (S₂O₈²⁻) ion by oxidation of SO₄²⁻ ion from the electrolyte by reaction (13) and ozone by reaction (14) [14,15].



It is important to remark that the oxidants produced in solution can also suffer chemical activation by irradiation (photocatalysis) and after that, other strong oxidant species can be produced by the combination of the oxidants produced with another species that leads to the production of very reactive species such as ozone and sulfate ion-radical. However, the undesired effect can be also observed because the effectiveness of the process could be reduced with a decrease of \bullet OH concentration due to its combination by reaction (10).

Fig. 3b depicts that the increase in j accelerates the antibiotic abatement, which disappears in 27, 13 and 11 min for 33.3, 66.6 and 100 mA cm⁻². The inset panel of this figure presents the excellent linear correlations obtained from the analysis of such substrate decays for a pseudo-first-order kinetics, giving rise to increasing k_1

Table 1

Products and hydroxylated derivatives identified by LC-MS during chloramphenicol degradation by EF in a BDD/air-diffusion tank reactor.

Product	Chemical name	-OH groups added	<i>m/z</i> ^a	<i>t_r</i> ^b (min)
1	Chloramphenicol	–	321 323 325 353 355 357	9.917 8.500
2	2,2-Dichloro-N-[1,3-dihydroxy-1-(4-hydroxyphenyl)propan-2-yl]acetamide	2	324 326 328	9.850
3	4-(2-Amino-1,3-dihydroxy-propanyl)-nitrobenzene	– 1 2	211 227 243	– 11.250 9.500
4	4-(2-Amino-1,3-dihydroxy-propanyl)-phenol	– 3	182 230	13.125 9.135
5	4-(2-Nitro-1,3-dihydroxy-propanyl)-nitrobenzene	– 2 3	241 273 289	15.083 8.653 9.305
6	4-Nitro-(2R)-hydroxy(phenyl)ethanoic acid	– 1 2	212 228 244	8.430 13.466 9.325
7	4-Hydroxy-(2R)-hydroxy(phenyl)ethanoic acid	–	183	8.341
8	4-Nitrobenzoic acid	– 1 4	166 182 230	7.020 13.041 9.033
9	4-Hydroxybenzoic acid	– 1 2 4	137 153 169 201	6.500 9.625 9.157 7.475
10	4-Nitrophenol	–	138	6.350
11	Dichloroacetic acid	–	127	7.568

^a Negative ion with *z* = 1.

^b Retention time.

values from 2.9×10^{-3} to $7.1 \times 10^{-3} \text{ s}^{-1}$ ($R^2 \sim 0.995\text{--}0.998$) when *j* changes from 33.3 to 100 mA cm $^{-2}$. This confirms the concomitant greater generation of •OH as the main oxidant of chloramphenicol.

The effect of substrate concentration on the oxidation ability of SPEF with BDD was explored for solutions containing 24.5–245 mg L $^{-1}$ of chloramphenicol at 33.3 mA cm $^{-2}$. For these trials, Fig. 4a evidences that total mineralization (98% DOC abatement) was achieved at a similar time of 120 min in all cases. That means that the mineralization rate was accelerated at higher chloramphenicol concentration, thereby making the process more efficient. This behavior can be seen in the inset panel of Fig. 4a, where the maximum MCE values gradually increased from 12% for 24.5 mg L $^{-1}$ to 100% for 245 mg L $^{-1}$. This suggests a progressive inhibition of parasitic reactions (9)–(14) to favor the attack of a larger proportion of BDD(•OH) and •OH on greater amounts of organics that are more rapidly mineralized and/or more quickly photolyzed by sunlight. The determination of substrate decay in these trials revealed that it disappeared at longer time at greater concentration, from 4 to 27 min, as depicted in Fig. 4b. Its inset panel evidences that chloramphenicol always followed a pseudo-first-order reaction, with decreasing *k*₁ values of $1.5 \times 10^{-2} \text{ s}^{-1}$ ($R^2 = 0.985$), $8.0 \times 10^{-3} \text{ s}^{-1}$ ($R^2 = 0.997$), $7.6 \times 10^{-3} \text{ s}^{-1}$ ($R^2 = 0.988$), $3.7 \times 10^{-3} \text{ s}^{-1}$ ($R^2 = 0.999$) and $2.9 \times 10^{-3} \text{ s}^{-1}$ ($R^2 = 0.998$) for increasing contents of 24.5, 61.2, 122.5, 183.7 and 245 mg L $^{-1}$. Note that the large drop in *k*₁ as chloramphenicol concentration rises is a surprising trend for a pseudo-first-order kinetics, since a rate constant independent of substrate content is theoretically expected. This may be related to the very short lifetime of hydroxyl radicals (about $4 \times 10^{-9} \text{ s}$) [44] which need to be continuously produced from water oxidation by reaction (3) and Fenton's reaction (4) with participation of H₂O₂ and Fe²⁺. The diffusion of all these species in the medium and their mass transport toward/from the electrodes then seem to limit the generation of BDD(•OH) and •OH giving a different constant concentration of them to attack chloramphenicol in each

trial. This could explain that its decay always follows a pseudo-first-order kinetics but with a *k*₁ value depending on the experimental variables tested.

The aforementioned findings highlight the great oxidation ability of BDD(•OH), •OH and sunlight in SPEF with BDD, allowing the complete mineralization of acidic waters polluted with high contents of chloramphenicol. The efficiency of this EAOP improves with decreasing *j* and rising substrate content.

3.3. Identification and evolution of oxidation products

Since hydroxyl radicals (Pt(•OH), BDD(•OH) and •OH) are the main oxidants in the EAOPs tested, the same products are expected to be formed in all them. The primary intermediates were then detected from short electrolysis times of a solution with 245 mg L $^{-1}$ chloramphenicol under EF with BDD at 33.3 mA cm $^{-2}$ by liquid chromatography-mass spectrometry (LC-MS). Table 1 summarizes the products identified by this technique and their main characteristics. Apart from chloramphenicol (1), nine aromatic products (2–10) and thirteen hydroxylated derivatives along with dichloroacetic acid (11) were found.

The cleavage of the benzenic ring of aromatic products and the degradation of their lateral groups are expected to form short-chain carboxylic acids [12,16,18,28–32]. Ion-exclusion HPLC of all treated solutions revealed the generation of tartaric (12, *t_r* = 8.24 min), maleic (13, *t_r* = 8.51 min), acetic (14, *t_r* = 14.96 min), oxalic (15, *t_r* = 7.00 min), oxamic (16, *t_r* = 9.39 min) and formic (17, *t_r* = 13.68 min) acids. Oxidation of tartaric, maleic and acetic acids yields oxalic and formic acids [12,16], whereas oxamic acid can be formed from precedent amino compounds. Besides, oxalic, oxamic and formic acids are ultimate carboxylic acids since they are directly oxidized to CO₂ [16,45].

The evolution of detected carboxylic acids was determined for the treatment of a 245 mg L $^{-1}$ chloramphenicol solution by

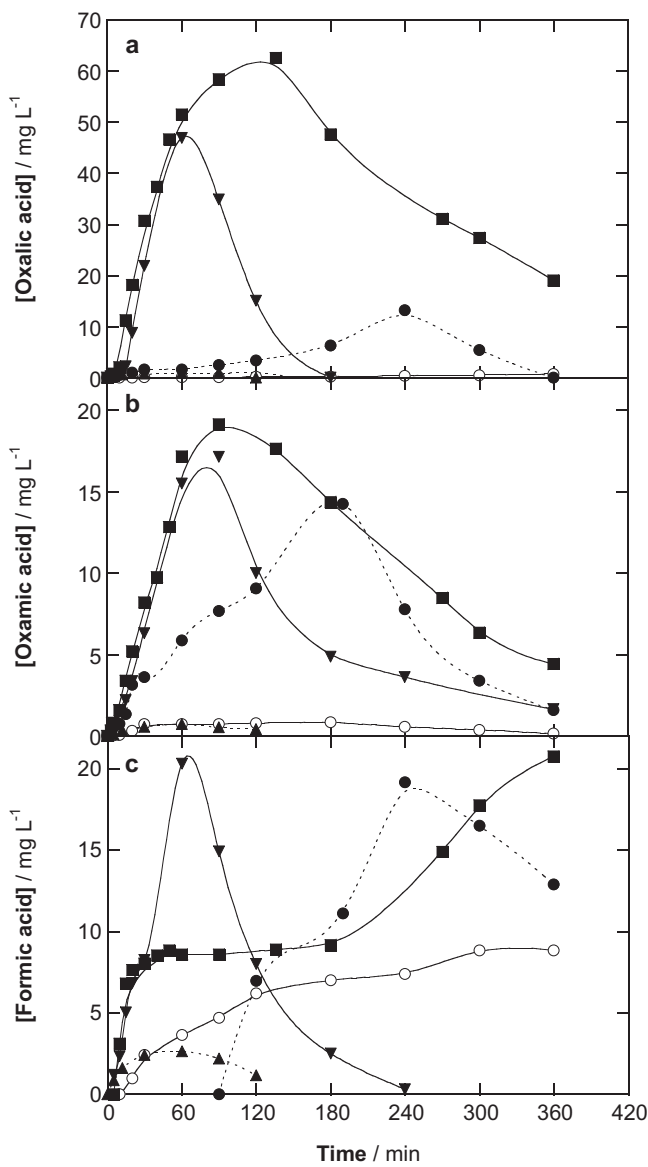


Fig. 5. Evolution of the concentration of (a) oxalic (**15**), (b) oxamic (**16**) and (c) formic (**17**) acids detected during the treatments of Fig. 1. Method: (○) AO- H_2O_2 with Pt, (●) AO- H_2O_2 with BDD, (■) EF with BDD, (▼) PEF with BDD and (▲) SPEF with BDD.

AO- H_2O_2 with Pt and BDD as well as EF, PEF and SPEF with BDD at 33.3 mA cm^{-2} . While only traces of **12–14** were found for the three latter methods, up to 8 mg L^{-1} of **12** were formed and completely removed at 360 min of both AO- H_2O_2 processes and **13** was continuously accumulated up to 2 mg L^{-1} in AO- H_2O_2 with Pt, being totally destroyed when using BDD. A very different behavior was obtained for the ultimate acids **15–17**, as shown in Fig. 5a–c. Thus, in AO- H_2O_2 with Pt, **15** and **16** were poorly produced ($<0.8\text{ mg L}^{-1}$) and up to 7.4 mg L^{-1} of **17** were continuously accumulated, according to the scarce DOC decay of this EAOP (see Fig. 1a). In contrast, the higher oxidation ability of AO- H_2O_2 with BDD allowed the faster destruction of precedent intermediates with larger accumulation of these three acids, which were also mineralized by BDD($\bullet OH$) at long electrolysis time, primordially **15** and **16**. The quicker destruction of aromatic products by $\bullet OH$ in EF with BDD favored the faster generation of the ultimate acids attaining maximum contents of 58.3 mg L^{-1} for **15**, 19.1 mg L^{-1} for **16** and 20.7 mg L^{-1} for **17**. Results of Fig. 5a–c evidence that Fe(III)-oxalate and Fe(III)-oxamate complexes were slowly removed from the attack of BDD($\bullet OH$) [16,45].

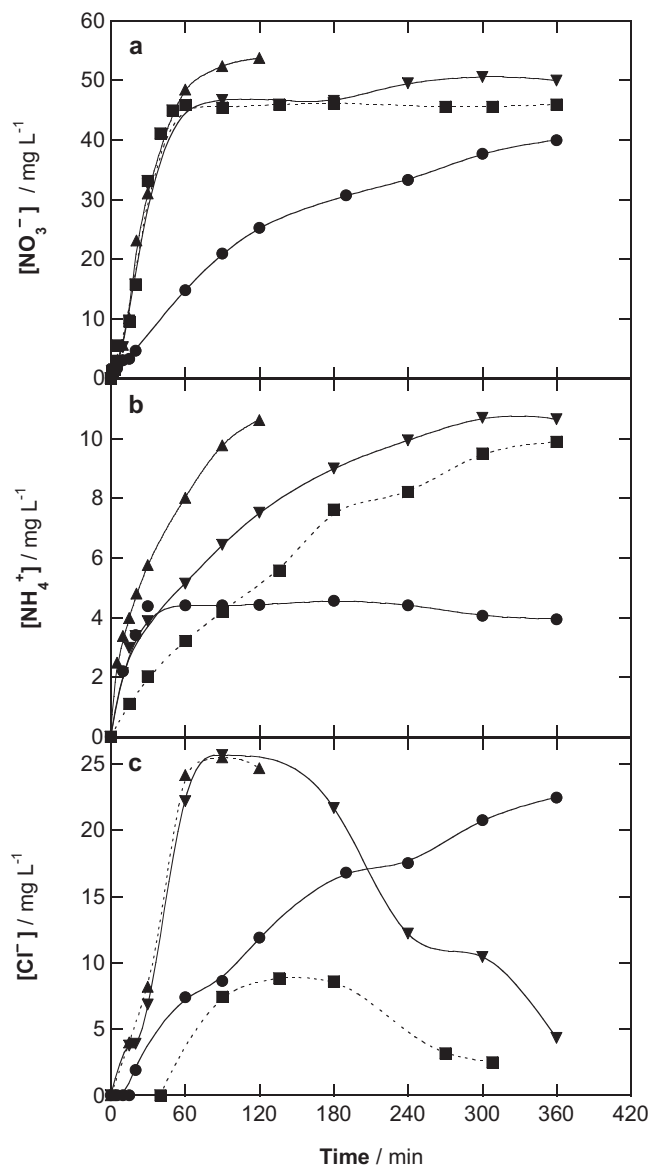


Fig. 6. Time-course of the concentration of: (a) nitrate, (b) ammonium and (c) chloride ions released during the degradations of Fig. 1 using a BDD/air-diffusion tank reactor. Method: (●) AO- H_2O_2 , (■) EF, (▼) PEF and (▲) SPEF.

whereas Fe(III)-formate species were more stable in solution. When PEF with BDD was used, these three Fe(III)-carboxylate complexes were rapidly photomineralized by UVA light from reaction (6), a process so rapid in SPEF with BDD that they were not practically accumulated. A simple mass balance at 120–135 min of AO- H_2O_2 , EF, PEF and SPEF with BDD indicated that the ultimate acids contributed in 5.2 , 23.2 , 10.0 and 0.76 mg L^{-1} DOC, respectively, related to 7.4% , 68% , 59% and 38% of the organic matter contained in the final treated solution. All these results confirm the preponderant attack of $\bullet OH$ on aromatic products to produce carboxylic acids, which can be slowly decayed by BDD($\bullet OH$) and the potent photolytic action of sunlight quickly mineralizes Fe(III)-carboxylate complexes. This explains the highest oxidation ability of SPEF with BDD than the other EAOPs.

The conversion of the initial N of chloramphenicol (21.2 mg L^{-1}) into NO_3^- and NH_4^+ ions in the treatments with BDD was assessed by ion chromatography. Fig. 6a and b shows that NO_3^- ion was formed usually more rapidly and always in larger extent, as proposed in reaction (8). At the end of electrolyses, 40 mg L^{-1}

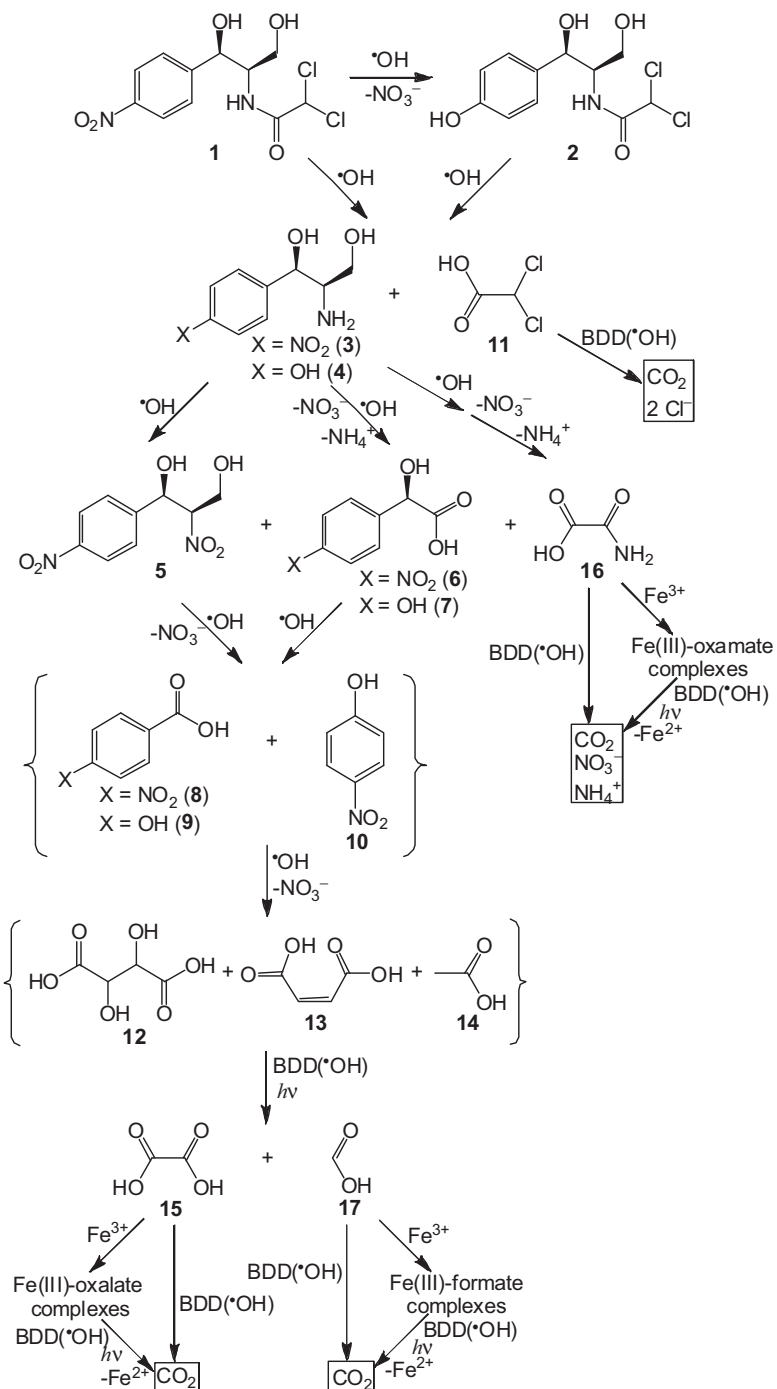


Fig. 7. General reaction sequence proposed for chloramphenicol mineralization by EAOPs in acidic aqueous medium.

NO₃⁻ (42% of initial N) and 4.1 mg L⁻¹ NH₄⁺ (15% of initial N) for AO-H₂O₂, 46 mg L⁻¹ NO₃⁻ (49% of initial N) and 9.9 mg L⁻¹ NH₄⁺ (36% of initial N) for EF, 50 mg L⁻¹ NO₃⁻ (53% of initial N) and 10.7 mg L⁻¹ NH₄⁺ (40% of initial N) for PEF and 54 mg L⁻¹ NO₃⁻ (59% of initial N) and 10.7 mg L⁻¹ NH₄⁺ (40% of initial N) for SPEF were found. TN analysis of the final solution treated by AO-H₂O₂ revealed the presence of 61% of the initial N, in good agreement with 57% of initial N related to the sum of NO₃⁻ and NH₄⁺ contents. This suggests the release of volatile N-derivatives in this process due to the smaller oxidation ability of BDD(•OH). The quicker oxidation of intermediates with •OH then favored their mineralization with larger release of inorganic ions, even enhanced under UVA and solar radiation.

TN measurements then confirmed the presence of the initial N as NO₃⁻ and NH₄⁺ ions in the final solution of the SPEF process. On the other hand, Fig. 6c shows that Cl⁻ ion was lost during the same trials, without reaching the initial Cl content of 53.7 mg L⁻¹. This ion was slowly accumulated in AO-H₂O₂ up to 24.7 mg L⁻¹ since it was slowly generated from the BDD(•OH) attack on chloro-organics and oxidized to chlorine at the BDD anode [14,28]. This phenomenon can be better observed for both EF and PEF processes, where Cl⁻ ion was much more rapidly released due to the greater oxidation ability of •OH and practically disappeared in 360 min. That means that Cl⁻ ion is a primary inorganic ion formed in chloramphenicol mineralization, as stated in reaction (8).

3.4. Reaction sequence for chloramphenicol mineralization

Fig. 7 presents a general reaction pathway for chloramphenicol mineralization by the EAOPs tested. Only the detected aromatic species have been considered, but not their hydroxylated derivatives for sake of simplicity. These compounds are assumed to be mainly oxidized by •OH in EF, PEF and SPEF, although their slower destruction with either Pt(•OH) or BDD(•OH) takes place in the AO-H₂O₂ processes.

The sequence is initiated by the hydroxylation with denitration of **1** to give **2**, along with the hydroxylation of these two compounds yielding **3** and **4** with loss of **11**, which is mineralized with release of Cl⁻ ions. Further oxidation of the amino group of **3** to nitro group leads to **5**, whereas deamination of the lateral group of **3** and **4** gives the aromatics **6** and **7** and their parallel degradation leads to acid **16**. Subsequent oxidation of the lateral groups of **6** and **7** gives compounds **8–10**. The cleavage of the benzenic ring of the above aromatics and the destruction of their lateral groups yields the mixture of acids **12–14**, which are further transformed into **15** and **17**. All short-chain carboxylic acids can be slowly removed under the action of BDD(•OH) in AO-H₂O₂ with BDD, whereas in EF, PEF and SPEF they form Fe(III)-carboxylate species that are also slowly destroyed by BDD(•OH) but much more rapidly photolyzed by UVA and solar radiation in the two latter EAOPs. These alternative reactions are indicated for the ultimate acids **15–17** that are directly converted into CO₂. Acid **16** also releases NO₃⁻ and NH₄⁺ ions during mineralization [45].

3.5. SPEF degradation with Pt in the solar pre-pilot plant

The most potent SPEF process was further scaled-up to a solar pre-pilot plant in order to assess its viability at industrial scale. A Pt anode was used to obtain a more economic process since gave a lower potential difference of the cell than using a BDD one. The pre-pilot plant then contained a Pt/air-diffusion filter-press cell coupled to the solar CPCs photoreactor. 10 L of 245 mg L⁻¹ chloramphenicol with 0.05 M Na₂SO₄ and 0.5 mM Fe²⁺ at pH 3.0 and 35 °C were treated in batch circulation mode by applying up to 100 mA cm⁻² and liquid flow rate of 200 L h⁻¹. Comparative EF in the dark was made to clarify the effect of irradiated sunlight.

As expected, the mineralization rate of the EF and SPEF processes increased when *j* rose. **Fig. 8a** exemplifies the normalized DOC decay found for 100 mA cm⁻². While DOC was slowly removed by EF only yielding 45% reduction in 360 min, it decayed much more rapidly by SPEF, being reduced by 89% in 180 min. This evidences the large synergistic action of sunlight using the CPCs photoreactor in SPEF. Besides, maximum MCE values of 19% for EF and 49% for SPEF were attained after 120 min of electrolysis, as can be seen in **Fig. 8b**. Comparison of these results with the total mineralization achieved at 180 min of SPEF at 33.3 mA cm⁻² with maximum efficiency of 80% using the stirred tank reactor (see **Fig. 1**) allows concluding that the SPEF process is viable in the solar pre-pilot plant, although it has lower oxidation ability to mineralize chloramphenicol.

For the above trials, the energy cost per unit DOC mass removed (EC_{DOC}) was calculated from Eq. (15) [42,43]:

$$\text{EC}_{\text{DOC}} \left(\text{kWh g}^{-1} \text{DOC} \right) = \frac{E_{\text{cell}} It}{V_s \Delta(\text{DOC})_{\text{exp}}} \quad (15)$$

where *E*_{cell} is the average potential difference of the cell (11.4 V), *I* is the applied current (9 A), *t* is the electrolysis time (h), *V*_s is the solution volume (L) and $\Delta(\text{DOC})_{\text{exp}}$ is the experimental DOC abatement (mg L⁻¹). **Fig. 8c** shows that the SPEF process was much more economic than the EF one. In both EAOPs, EC_{DOC} dropped from the starting of electrolysis reaching minimal of 0.676 and 0.255 kWh g⁻¹ DOC after 2 h of EF and SPEF, respectively, just when

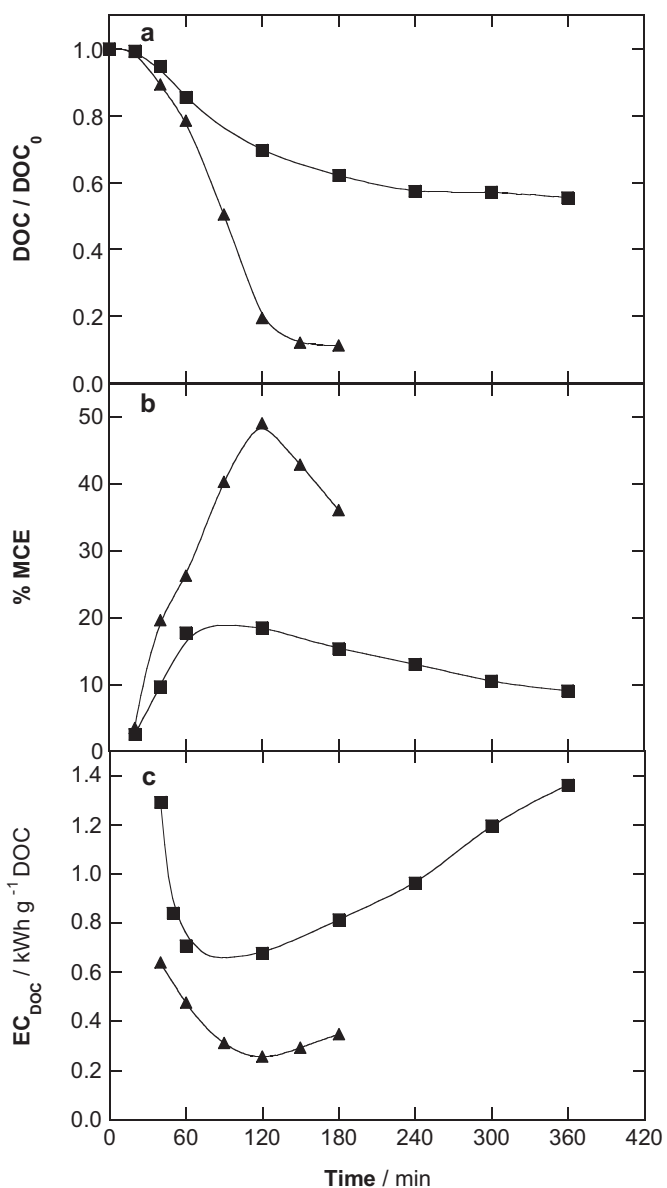


Fig. 8. Change of (a) normalized DOC, (b) mineralization current efficiency and (c) energy consumption per unit DOC mass for the (■) EF (in the dark) and (▲) SPEF treatments of a 245 mg L⁻¹ chloramphenicol solution in 0.05 M Na₂SO₄ with 0.5 mM Fe²⁺ at pH 3.0, 100 mA cm⁻² and 35 °C in the 10 L pre-pilot plant containing a Pt/air-diffusion filter-press reactor coupled to a solar CPCs photoreactor at liquid flow rate of 200 L h⁻¹.

their best efficiencies were attained (see **Fig. 8b**). At the end of SPEF (180 min), an EC_{DOC} value of 0.347 kWh g⁻¹ DOC related to 30.8 kWh m⁻³ energy cost was obtained. Taking into account that the electrical energy cost of the Endesa, S.A., company in Spain is of about 0.141 € kWh⁻¹, one can estimate a cost of 4.35 € m⁻³ for the SPEF process. This low cost confirms its viability for possible application to industrial scale.

The chloramphenicol concentration decayed with similar rate in both EF and SPEF treatments, as can be seen in **Fig. 9**, where the antibiotic disappeared in about 60 min. The inset panel of this figure shows the excellent straight lines obtained considering a pseudo-first-order reaction, giving rise to *k*₁ values of 1.4×10^{-3} s⁻¹ (*R*² = 0.994) for EF and 1.6×10^{-3} s⁻¹ (*R*² = 0.994) for SPEF. This evidences again the small participation of photolytic reaction (5) to produce significant amounts of the main oxidant •OH in SPEF. The fact that a much greater *k*₁ value of 2.9×10^{-3} s⁻¹ was obtained

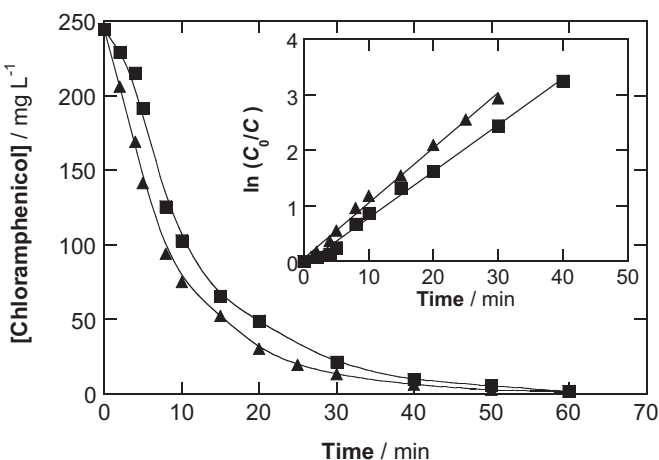


Fig. 9. Chloramphenicol concentration decay for the trials of Fig. 8. The inset panel presents the kinetic analysis assuming a pseudo-first-order reaction for the drug. Method: (■) EF and (▲) SPEF.

operating at lower j of 33.3 mA cm⁻² in the stirred tank reactor, corroborates the formation of lower amounts of •OH from Fenton's reaction (4) in the solar pre-pilot plant, thereby making the SPEF process with Pt less efficient.

The time course of generated carboxylic acids for SPEF with Pt is depicted in Fig. 10a. While acids **12**, **13** and **15** disappeared completely during the 180 min of electrolysis, high amounts of **16** (15 mg L⁻¹) together only 1.8 mg L⁻¹ of **14** and 2.6 mg L⁻¹ of **17**

remained in the solution. The amounts of these acids represent 5.5 mg L⁻¹ DOC, i.e., a 50% of the DOC present in the final solution (see Fig. 8a), then being their main components. The greater persistence of Fe(III)-carboxylate complexes in the solar pre-pilot plant compared to the stirred tank reactor can be related to the poorer capture of solar radiation by the solution volume. Thus, the 100 mL cell was totally irradiated by sunlight in contrast to the very low irradiated volume/total volume ratio of 15.7% used in the 10 L pre-pilot plant at liquid flow rate of 200 L h⁻¹. Nevertheless, the latter system had a better solar radiation capture system from CPCs, which can use efficiently direct and diffuse solar irradiation, whereas the stirred tank reactor mostly used the direct radiation, although a very small part of diffuse UV radiation reflected by the mirror at the bottom of the cell reached the solution.

On the other hand, Fig. 10b confirms the release of NO₃⁻, NH₄⁺ and Cl⁻ ions during the SPEF treatment with Pt. NO₃⁻ ion was preferentially formed, being accumulated up to 51 mg L⁻¹ (54% of initial N), whereas only 10 mg L⁻¹ (36% of initial N) of NH₄⁺ ion were formed. TN analysis of the final degraded solution confirmed that it contained all the initial N, which was distributed in the form of NO₃⁻ and NH₄⁺ ions (90%) and the remaining **16** (10%). This indicates again the high oxidation of this EAOP to mineralize all N-compounds. In contrast, Cl⁻ ion was continuously accumulated up to a maximum content of 46 mg L⁻¹ at about 150 min of electrolysis. This behavior differs from that found in the stirred tank reactor with a BDD anode (see Fig. 6c), suggesting a much slower destruction of chloroderivatives, like **11**, in the pre-pilot plant with a much slower oxidation of Cl⁻ ion to chlorine at the Pt anode.

4. Conclusions

It has been demonstrated that SPEF with BDD is the most potent EAOP for chloramphenicol mineralization at pH 3.0 using a 100 mL stirred BDD/air-diffusion tank reactor. Total mineralization of antibiotic solutions with 0.05 M Na₂SO₄ and 0.5 mM Fe²⁺ at pH 3.0 can be rapidly attained by the combined action of BDD(•OH), •OH and sunlight. PEF with BDD was less powerful due to the lower intensity of UVA radiation to photolyze generated Fe(III)-carboxylate species. EF and AO-H₂O₂ with BDD led to partial mineralization, the former being more potent because chloramphenicol and its aromatic products were more rapidly destroyed by •OH than BDD(•OH). Comparative treatments with a Pt anode yielded slower mineralization than using BDD because of the smaller oxidation ability of Pt(•OH), although total mineralization was also achieved for the SPEF process. In all these EAOPs, the antibiotic decayed following a pseudo-first-order reaction, with similar apparent constant rate in EF, PEF and SPEF since •OH formed from Fenton's reaction (4) was the main oxidant. For SPEF with BDD, the mineralization current efficiency was enhanced with decreasing j and increasing substrate concentration. The opposite trend was found for the apparent rate constant of the antibiotic decay. Nine aromatic products and thirteen hydroxylated derivatives were identified by LC-MS. Tartaric, maleic and acetic acids, along with oxalic, oxamic and formic as ultimate acids, were quantified by ion-exclusion HPLC. While the Fe(III)-carboxylate complexes of the three latter acids were slowly removed by BDD(•OH) in EF with BDD, they were rapidly photolyzed by UVA light in PEF with BDD and much more quickly photodecomposed by sunlight in SPEF with BDD. NO₃⁻ ion and, in smaller extent, NH₄⁺ ion were released in all processes. Cl⁻ ion was also lost, but it was oxidized to chlorine at the BDD anode surface. From the detected products, a plausible general reaction sequence for chloramphenicol mineralization by EAOPs is proposed. The SPEF process with Pt was viable when it was scaled-up to a 10 L solar pre-pilot plant. This system showed less oxidation ability than the 100 mL stirred tank reactor, leading to partial

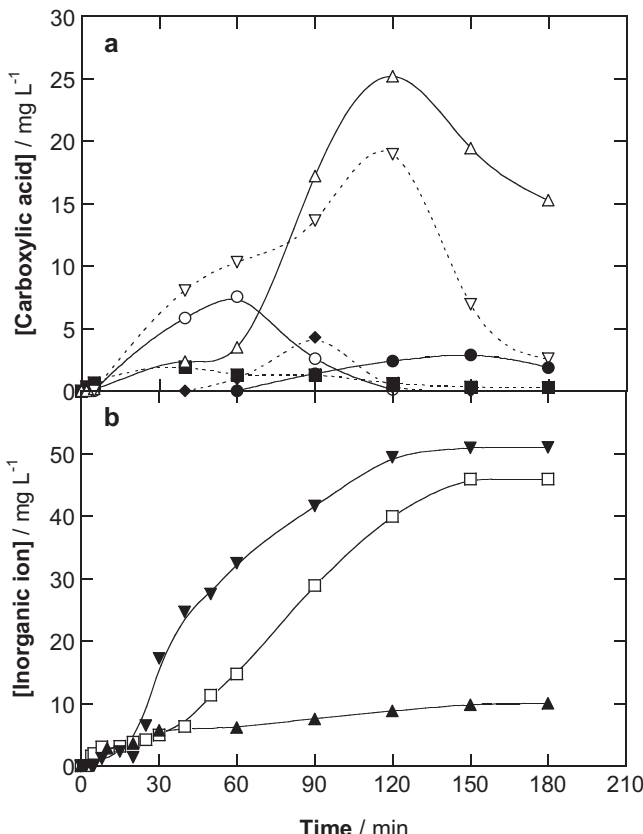


Fig. 10. Evolution of the concentration of (a) carboxylic acids and (b) inorganic ions formed during the experiment of Fig. 8 with a Pt/air-diffusion filter-press reactor. In plot (a), (◆) tartaric (**12**), (■) maleic (**13**), (●) acetic (**14**), (○) oxalic (**15**), (△) oxamic (**16**) and (▽) formic (**17**) acids. In plot (b), (▼) nitrate, (▲) ammonium and (□) chloride ions.

mineralization of a 245 mg L⁻¹ antibiotic solution. After 180 min of electrolysis at 100 mA cm⁻² and liquid flow rate of 200 L h⁻¹, 89% mineralization with 36% current efficiency and 30.8 kWh m⁻³ energy cost was obtained. Acetic, formic and primordially oxamic acids were the main components remaining in the final solution because of the poorer capture of solar radiation by the solution volume.

Acknowledgments

The authors gratefully acknowledge the financial support from MICINN (Ministerio de Ciencia e Innovación, Spain) under the Project CTQ2010-16164/BQU, co-financed with FEDER funds. S. Garcia-Segura thanks the grant awarded from MEC (Ministerio de Educación y Ciencia, Spain) and E.B. Cavalcanti acknowledges the financial support from CAPES/MEC/Brazil and Universidade Tiradentes/UNIT.

References

- [1] K. Kümmeler, Chemosphere 75 (2009) 417–434.
- [2] K. McClellan, R.U. Halden, Water Res. 44 (2010) 6011–6020.
- [3] L.-J. Zhou, G.-G. Ying, S. Liu, J.-L. Zhao, B. Yang, Z.-F. Chen, H.-J. Lai, Sci. Total Environ. 452–453 (2013) 365–376.
- [4] I. Kim, N. Yamashita, H. Tanaka, J. Hazard. Mater. 166 (2009) 1134–1140.
- [5] V. Homem, L. Santos, J. Environ. Manage. 92 (2011) 2304–2347.
- [6] P. Verlicchi, A. Galletti, M. Petrovic, D. Barceló, M. Al Aukidy, E. Zambello, Sci. Total Environ. 454–455 (2013) 411–425.
- [7] Y. Xu, F. Luo, A. Pal, K.Y.-H. Gin, M. Reinhard, Chemosphere 83 (2011) 963–969.
- [8] H.W. Leung, T.B. Minh, M.B. Murphy, J.C.W. Lam, M.K. So, M. Martin, P.K.S. Lam, J.B. Richardson, Environ. Int. 42 (2012) 1–9.
- [9] R. Andreozzi, V. Caprio, C. Ciniglia, M. De Campore, R. Lo Giudice, R. Marotta, E. Zuccato, Environ. Sci. Technol. 38 (2004) 6832–6838.
- [10] M. Crane, C. Watts, T. Boucard, Sci. Total Environ. 367 (2006) 23–41.
- [11] F. Pomati, C. Orlandi, M. Clerici, F. Luciani, E. Zuccato, Toxicol. Sci. 102 (2008) 129–137.
- [12] I. Sirés, E. Brillas, Environ. Int. 40 (2012) 212–229.
- [13] C.A. Martínez-Huitile, S. Ferro, Chem. Soc. Rev. 35 (2006) 1324–1340.
- [14] C.A. Martínez-Huitile, E. Brillas, Angew. Chem. Int. Ed. 47 (2008) 1998–2005.
- [15] M. Panizza, G. Cerisola, Chem. Rev. 109 (2009) 6541–6569.
- [16] E. Brillas, I. Sirés, M.A. Oturan, Chem. Rev. 109 (2009) 6570–6631.
- [17] M. Klavarioti, D. Mantzavinos, D. Kassinos, Environ. Int. 35 (2009) 402–417.
- [18] A. Özcan, Y. Sahin, A. Savas Koparal, M.A. Oturan, J. Electroanal. Chem. 616 (2008) 71–78.
- [19] M. Zarei, A.R. Khataee, R. Ordikhani-Seyedlar, M. Fathinia, Electrochim. Acta 55 (2010) 7259–7265.
- [20] M. Zarei, A. Niaezi, D. Salari, A.R. Khataee, J. Hazard. Mater. 173 (2010) 544–551.
- [21] I. Sirés, J.A. Garrido, R.M. Rodríguez, E. Brillas, N. Oturan, M.A. Oturan, Appl. Catal. B: Environ. 72 (2007) 382–394.
- [22] I. Sirés, N. Oturan, M.A. Oturan, R.M. Rodríguez, J.A. Garrido, E. Brillas, Electrochim. Acta 52 (2007) 5493–5503.
- [23] A. Ozcan, Y. Sahin, A.S. Koparal, M.A. Oturan, J. Hazard. Mater. 153 (2008) 718–727.
- [24] A. Dirany, S. Efremova-Aaron, N. Oturan, I. Sirés, M.A. Oturan, J.-J. Aaron, Anal. Bioanal. Chem. 400 (2011) 353–360.
- [25] A. Dirany, I. Sirés, N. Oturan, A. Özcan, M.A. Oturan, Environ. Sci. Technol. 46 (2012) 4074–4082.
- [26] M. Panizza, M.A. Oturan, Electrochim. Acta 56 (2011) 7084–7087.
- [27] K. Cruz-González, O. Torres-López, A. García-León, J.L. Guzmán-Mar, L.H. Reyes, A. Hernández-Ramírez, J.M. Peralta-Hernández, Chem. Eng. J. 160 (2010) 199–206.
- [28] I. Sirés, F. Centellas, J.A. Garrido, R.M. Rodríguez, C. Arias, P.L. Cabot, E. Brillas, Appl. Catal. B: Environ. 72 (2007) 373–381.
- [29] E. Guinea, J.A. Garrido, R.M. Rodríguez, P.L. Cabot, C. Arias, F. Centellas, E. Brillas, Electrochim. Acta 55 (2010) 2101–2115.
- [30] S. Garcia-Segura, J.A. Garrido, R.M. Rodríguez, P.L. Cabot, F. Centellas, C. Arias, E. Brillas, Water Res. 46 (2012) 2067–2076.
- [31] A. El-Ghenemy, P.L. Cabot, F. Centellas, J.A. Garrido, R.M. Rodríguez, C. Arias, E. Brillas, Chemosphere 91 (2013) 1324–1331.
- [32] E.B. Cavalcanti, S. Garcia-Segura, F. Centellas, E. Brillas, Water Res. 47 (2013) 1803–1815.
- [33] B. Kasprzyk-Hordern, R.M. Dinsdale, A.J. Guwy, Water Res. 42 (2008) 3498–3518.
- [34] L. Tong, W. Ping, Y. Wang, K. Zhu, Chemosphere 74 (2009) 1090–1097.
- [35] A.I. Okoh, E.O. Igbinosa, BMC Microbiol. 10 (2010) 143.
- [36] H. Xu, W. Chen, C. Wang, J. Yang, L. Zhao, Fres. Environ. Bull. 21 (2012) 1619–1625.
- [37] V. Suling, J. Wohlers, M. Reinhard, W. Thiemann, Vom Wasser 98 (2002) 145–158.
- [38] A. Chatzitakis, C. Berberidou, I. Paspaltsis, G. Kyriakou, T. Sklaviadis, I. Poulios, Water Res. 42 (2008) 386–394.
- [39] J. Wang, W. Sun, C. Xu, W. Liu, Int. J. Environ. Technol. Manage. 15 (2012) 180–192.
- [40] M. Feng, D. Long, Y. Fang, Anal. Chim. Acta 363 (1998) 67–73.
- [41] E. Brillas, M.A. Baños, S. Camps, C. Arias, P.L. Cabot, J.A. Garrido, R.M. Rodríguez, New J. Chem. 28 (2004) 314–322.
- [42] L.C. Almeida, S. Garcia-Segura, N. Bocchi, E. Brillas, Appl. Catal. B: Environ. 103 (2011) 21–30.
- [43] E.J. Ruiz, C. Arias, E. Brillas, A. Hernández-Ramírez, J.M. Peralta-Hernández, Chemosphere 82 (2011) 495–501.
- [44] R. Roots, S. Okada, Radiat. Res. 64 (1975) 306–320.
- [45] S. Garcia-Segura, E. Brillas, Water Res. 45 (2011) 2975–2984.